의학박사 학위논문

A novel direct activation mechanism of TRPC4 and TRPC5 channels by selective $G\alpha_i$ subunits

$G\alpha_i$ 아형 단백질에 의한 TRPC4와 TRPC5 이온통로의 활성화 기전에 관한 연구

2012년 8월

서울대학교 대학원
의과학과 의과학전공

전 재 표

$G\alpha_i$ 아형 단백질에 의한 TRPC4와 TRPC5 이온통로의 활성화 기전에 관한 연구

지도교수 서 인 석

이 논문을 의학 박사 학위논문으로 제출함

2012년 4월

서울대학교 대학원

의과학과 의과학 전공

전 재 표

전재표의 의학박사 학위논문을 인준함

2012년 7월

위 원 장 _____(인)

부위원장 _____(인)

위 원 _____(인)

위 원 _____(인)

위 원 _____(인)

A novel direct activation mechanism of TRPC4 and TRPC5 channels by selective $G\alpha_i$ subunits

by

Jae-Pyo Jeon

A Thesis Submitted to the Department of Biomedical Sciences in Partial Fulfillment of the Requirements for the Degree of Doctor of Philosophy in Medical Science (Biomedical Sciences) at the Seoul National University College of Medicine

July 2012

Approved by thesis committee:

Professor _____ (Chairman)

Professor _____ (Vice chairman)

Professor _____

Professor _____

Professor _____

학위논문 원문제공 서비스에 대한 동의서

본인의 학위논문에 대하여 서울대학교가 아래와 같이 학위논문 저작물을 제 공하는 것에 동의합니다.

1. 동의사항

① 본인의 논문을 보존이나 인터넷 등을 통한 온라인 서비스 목적으로 복제할 경우 저작물의 내용을 변경하지 않는 범위 내에서의 복제를 허용합니다.

② 본인의 논문을 디지털화하여 인터넷 등 정보통신망을 통한 논문의 일부 또는 전부의 복제.배포 및 전송 시 무료로 제공하는 것에 동의합니다.

2. 개인(저작자)의 의무

본 논문의 저작권을 타인에게 양도하거나 또는 출판을 허락하는 등 동의 내용을 변경하고자 할 때는 소속대학(원)에 공개의 유보 또는 해지를 즉시 통보하겠습니다.

3. 서울대학교의 의무

① 서울대학교는 본 논문을 외부에 제공할 경우 저작권 보호장치(DRM)를 사용하여야 합니다.

② 서울대학교는 본 논문에 대한 공개의 유보나 해지 신청 시 즉시 처리해야 합니다.

논문제목 : A novel direct activation mechanism of TRPC4 and TRPC5 channels by Selective $G\alpha_i$ subunits

학위구분 : **석사 □. 박사 □**

학 과 : 의과학과

학 번 : 2009-30610

연 락 처 :

저 작 자 : 전 재 표(인)

제 출 일 : 2012년 8월 일

서울대학교총장 귀하

Abstract

A novel direct activation mechanism of TRPC4 and TRPC5 channels by selective $G\alpha_i$ subunits

Jae-Pyo Jeon
Department of Biomedical Sciences
Seoul National University Graduate School

The Transient Receptor Potential Canonical (TRPC) channels function as non-selective, Ca^{2+}-permeable channels and mediate numerous cellular functions. It is commonly assumed that TRPC channels are activated by stimulation of $G\alpha_q$-PLC-coupled receptors. However, whether the $G\alpha_q$-PLC pathway is the main regulator of TRPC4/5 channels and how other $G\alpha$ proteins may regulate these channels are poorly understood. We previously reported that TRPC4/TRPC5 can be activated by $G\alpha_i$. In the current work, we found that $G\alpha_i$ subunits, rather than $G\alpha_q$, are the primary and direct activators of TRPC4 and TRPC5. We report a novel molecular mechanism in which TRPC4 is activated by several $G\alpha_i$ subunits, most prominently by $G\alpha_{i2}$, and TRPC5 is activated primarily by $G\alpha_{i3}$. Activation of $G\alpha_i$ by the muscarinic M2 receptors or expression of the constitutively active $G\alpha_i$ mutants equally and fully activates the channels. Moreover, both TRPC4 and TRPC5 are activated by direct interaction of their conserved C-terminal SEC14-like and spectrin-type domains (SESTD) with the $G\alpha_i$ subunits. Two amino acids (lysine 715 and arginine 716) of the TRPC4 C-terminus were identified by structural modeling as mediating the interaction with $G\alpha_{i2}$. These findings indicate an essential role of $G\alpha_i$ proteins as novel activators for TRPC4/5 and reveal the molecular mechanism by which G proteins activate the channels.

* This work is published in The Journal of biological chemistry (2012; 287:17029-39).

……

……

keywords : TRPC, TRPC4, TRPC5, $G\alpha_{i2}$, $G\alpha_{i3}$

Student Number **: 2009-30610**

List of figures

Contents

Introduction

Transient Receptor Potential Canonical (TRPC) channels are considered the molecular candidates for receptor-operated Ca^{2+}-permeable cation channels. The G-protein-coupled receptor (GPCR)-$G\alpha_q$-PLC is assumed to be the primary pathway for activation of all TRPC channels, even though the exact mechanism by which the channels are activated remains unknown (Schaefer et al, 2000). Several mediators have been proposed to mediate channel activation by stimulation of GPCR. Among them are SESTD1 (Miehe et al, 2010), intracellular Ca^{2+} (Blair et al, 2009; Gross et al, 2009), lipid metabolites (Flemming et al, 2005; Xu et al, 2006), PIP_2 (Kim et al, 2008; Otsuguro et al, 2008; Trebak et al, 2009), calmodulin (Tang et al, 2001; Ordaz et al, 2005), CaMK (Shi et al, 2004), MLCK (Kim et al 2006; Kim et al, 2007; Shimizu et al, 2006), and channel exocytosis (Bezzerides et al, 2004). In addition, TRPC4 and TRPC5 can be activated by thioredoxin (Xu et al, 2008) and NO (Yoshida et al, 2006).

The physiological role of these channels was established recently, demonstrating that TRPC4 and TRPC6 are the molecular candidates for the non-selective cation channels activated by muscarinic receptor stimulation (mI_{CAT}) in visceral smooth muscle cells. mI_{CAT} mediates the physiological action of acetylcholine in evoking smooth muscle contraction (So et al, 2003). Activation of muscarinic receptors causes the opening of non-selective cationic channels in smooth muscle cells of the gastrointestinal tract (Lee et al, 2005; Tsvilovskyy et al, 2009). In these cells, PTX-sensitive G proteins but not $G\beta\gamma$ were suggested to mediate channel activation (Kim et 1998; Yan et al,

2003). At the level of M2 or M3 muscarinic receptors, Sakamoto et al. (Sakamoto et al, 2007) showed three distinct signaling pathways that activate cationic channels in murine gut smooth muscle cells. The three pathways include the M2, M3, and M2/M3 pathways and were demonstrated using M2 k/o, M3 k/o, and M2/M3 double k/o mice, respectively. In addition, the M2/M3 pathway but not the M2 or M3 pathways involves processes in which Ca^{2+} has a potentiating effect on channel activation, suggesting that the M3 pathway may facilitate the function of the M2/M3 pathway through IP_3-induced Ca^{2+} release (Sakamoto et al, 2007). Similarly, activation of m*I*CAT requires the simultaneous activation of both the M2 and M3 muscarinic receptors (Lee et al, 2005), further suggesting involvement of $G\alpha_i$ in channel activation.

Several studies have also suggested that PTX-sensitive G-proteins play an important role in the activation process of TRPC4 and TRPC5 by GPCR (Xu et al, 2006; Otsuguro et al, 2008; Jeon et al, 2008). In our previous study, we showed that $G\alpha_{i2}$ activates TRPC4β and that PTX inhibits the activation of TRPC4β by stimulation of M2 muscarinic receptors (Jeon et al, 2008). However, the specificity for $G\alpha_i$ subunits and how the PTX-sensitive G-proteins activate the channels are not yet known; it is assumed that the PTX-sensitive G-proteins activate the channels by an indirect mechanism that involves the generation of second messengers. The well-known second messenger of PTX-sensitive G-proteins is cyclic AMP (cAMP), found downstream of adenylate cyclase (AC). PTX-sensitive G-proteins inhibit AC, which in turn decreases cAMP concentration. In our recent study, we showed that cAMP inhibits TRPC4/5 currents by activating PKA and phosphorylating

TRPC4 and TRPC5 channels (Sung et al, 2011). Thus, it cannot be the mechanism by which $G\alpha_i$ activates the channels.

These findings prompted us to ask whether TRPC4 and TRPC5 are activated by other PTX-sensitive $G\alpha_{i/o}$ subunits and whether the activation is direct. We were also interested in identifying the TRPC4 and TRPC5 domain that mediates the interaction with the channels and the activation by $G\alpha_{i/o}$ subunits, as well as the roles $G\alpha_q$ plays in modulating TRPC4 and TRPC5. In the present study, we focused on the role of $G\alpha_i$ proteins in regulating TRPC4/5 and report that $G\alpha_i$ subunits specifically activate TRPC4 and TRPC5 by direct interaction with the channels. Moreover, the regulation is specific to $G\alpha_i$ subunits. TRPC4 is mainly activated by $G\alpha_{i2}$, whereas TRPC5 is primarily activated by $G\alpha_{i3}$. These findings explain how TRPC4 is activated to regulate GI motility. Strategies can now be developed to understand the functional consequences of activation of TRPC4/5 in the central and peripheral nervous systems.

Material and Method

Cell Culture and Transient Transfection, cDNA clones

Human embryonic kidney (HEK293) cells (ATCC, USA) were maintained according to the supplier's recommendations. For transient transfection, cells were seeded in 12-well plates. The following day, 0.5 μg/well of pcDNA3 vector containing the cDNA for mouse TRPC4β was mixed with 50-100 ng/well of pEGFP-N1 (Clontech, USA) and transfected using the transfection reagent FuGENE 6 (Roche Applied Science, USA), as detailed in the manufacturer's protocol. Human TRPC5-EGFP cDNA and mouse TRPC4β-EGFP cDNA were also transfected in the same way. Coexpression of TRPC channels with G-proteins or receptors was achieved through a channel to G-protein transfection ratio of 1:1. After 30-40 h, the cells were trypsinized and transferred to a small recording chamber (RC-11, Warner Instruments, USA) for whole-cell recording. HEK293 cells stably expressing mouse TRPC4β were established by G418 selection. The cells were cultured as for the transient transfection, except that the medium was supplemented with G418 (400 μg/ml). Human $G\alpha_{i1}^{Q204L}$, $G\alpha_{i2}^{Q205L}$, $G\alpha_{i3}^{Q204L}$, rat $G\alpha_{i2}^{Q205L}$, and human $G\alpha_{q}^{Q209L}$ were cloned into pcDNA3.1+. Human $G\beta_{1,}$ $G\beta_{2}$, $G\beta_{3}$, $G\beta_{5,}$ and bovine $G\gamma_{2}$ were cloned into pcDNA3.1+ (Invitrogen, USA). Human $G\alpha_{oA}^{Q205L}$, M2 receptor (the Missouri S&T cDNA Resource Center (www.cdna.org), USA), and M3 receptor were cloned into pcDNA3.1+. Human $G\beta_{1}$ was used to insert the $G\beta_{1}^{W99A}$ and $G\beta_{1}^{I80A}$ mutations using the QuickChange site-directed mutagenesis kit (Stratagene, USA).

Western blotting and co-immunoprecipitation.

Transfected cells were collected and lysed using 300 μl of binding buffer (50 mM HEPES, pH 7.4, 120 mM NaCl, 2 mM EDTA, 2 mM $MgCl_2$, complete protease inhibitor mixture tablet, phosphatase inhibitor cocktail tablet (Roche Applied Science, USA) and 0.5% Triton X‑100). The lysates were sonicated, and any insoluble material was removed by centrifugation at 13,300 × *g* for 10 min. For co-immunoprecipitation of TRPC4β-GFP and TRPC5-GFP with $G\alpha_{i2}$ and $G\alpha_{i3}$, anti-GFP antibody (1 μg; A11122, Invitrogen, USA) was added to 100 μl cell extract and incubated for 12 h at 4 °C. Then, 50 μl of a 1:1 slurry of protein G Sepharose 4B beads was added to the antibody-extract mix and incubated for 12 h at 4 ºC. Beads were washed three times with binding buffer; proteins were released from the beads with 50 μl of 2 × SDS-loading buffer and analyzed with 10% or 8% SDS-PAGE. $G\alpha_{i2}$ and $G\alpha_{i3}$ were co-precipitated with GFP antibody and probed by mouse monoclonal anti-$G\alpha_{i2}$ antibody (2 μg; sc-13534, Santa Cruz, USA) and mouse monoclonal Anti-EE antibody for $G\alpha_{i3}$ (2 μg; MMS-115P, Covance, USA). The mouse monoclonal anti-$G\alpha_{i2}$ antibody was used for a reciprocal co-immunoprecipitation with GFP antibody in a sequential experiment. Co-immunoprecipitation of TRPC4β-GFP with $G\alpha_q$ was achieved using the same procedures. $G\alpha_q$ was probed by mouse monoclonal anti-$G\alpha_q$ antibody (sc-136181, Santa Cruz, USA).

Rat brain from day 15 was homogenized on ice using a Dounce homogenizer. The homogenate buffer had the same composition as the binding buffer. Homogenates were centrifuged at 13,000 rpm for 30 min at 4 ºC. Supernatants were re-centrifuged at 13,000 rpm at 4 ºC for 20 min. Supernatants were pre-

cleared with protein G sepharose beads for 1 hr at 4 ºC and centrifuged at 2000 rpm for 2 min at 4 ºC. Fifty microliters of a 1:1 slurry of protein G sepharose beads was added to the rabbit polyclonal antibody (Anti-$G\alpha_{i2}$; sc-7276, Santa Cruz, and anti-$G\alpha_{i3}$; sc-262, Santa Cruz, USA) extract mix and incubated for 12 hr at 4 ºC. The omission of primary antibody was used as a control. Beads were washed three times with binding buffer. Immunoprecipitated proteins were probed with Anti-TRPC4 (75-119, neuroMab, USA) and Anti-TRPC5 (75-104, neuroMab, USA) on an 8% SDS-PAGE gel. Anti-TRPC4 and Anti-TRPC5 were used for reciprocal pull downs. Controls were omission of the primary antibody and substitution of normal anti-mouse IgG with non-immune serum (sc-2025, Santa Cruz, USA). Rabbit polyclonal anti-$G\alpha_{i2}$ (2 μg; sc-7276, Santa Cruz, USA) and rabbit polyclonal anti-$G\alpha_{i3}$ (2 μg; sc-262, Santa Cruz, USA) antibodies were used to probe co-immunoprecipitation samples on a 10% SDS-PAGE gel.

Surface biotinylation.

Cells were washed with and suspended in PBS. Suspended cells were incubated in 0.5 mg/ml sulfo-NHS-LC-biotin (Pierce, USA) in PBS for 30 min on ice. Free biotin was quenched by the addition of 100 mM glycine in PBS. Lysates were prepared in lysis buffer by being passed 7-10 times through a 26-gauge needle after sonication. Lysates were centrifuged at 13,300 × *g* for 10 min at 4 °C, and protein concentrations of the supernatants were determined. Forty microliters of a 50% slurry of avidin beads (Pierce, USA) was added to cell lysates equivalent to 400 μg of protein. After incubation for 1 h at room temperature, beads were washed three times with

0.5% Triton X-100 in PBS, and proteins were extracted in sample buffer. Collected proteins were then analyzed by 8% SDS-PAGE gel and probed by anti-GFP antibody (A11122, Invitrogen, USA).

GST pull-down assays

The C-terminal domain of TRPC4 (621-890) was cloned into BamHI–SalI restriction sites of pGEX4T-1 (Amersham Biosciences, USA) by PCR. The GST fusion constructs were expressed and purified from *Escherichia coli* [BL21(DE3)]. Briefly, *Escherichia coli* were grown in liquid cultures containing 0.1 mM isopropyl-1-thio-h-galactopyranoside (IPTG) with vigorous agitation for 18 h at 20 C to an A600 of 0.6. Channel protein was purified from the soluble extract using glutathione-agarose beads (Amersham Biosciences, USA). GST fusion proteins appeared to be sensitive to degradation and carefully utilized in subsequent binding assays conducted within 24 h following purification. Histidine-tagged $G\alpha_{i2}^{Q205L}$ protein was expressed in *E. coli* [BL21(DE3)] from the pET15b plasmid containing full-length human $G\alpha_{i2}^{Q205L}$ cDNA. Histidine-tagged forms of $G\alpha_{i2}^{Q205L}$ were purified using immobilized Ni^{2+}-NTA affinity chromatography. Binding between $G\alpha_{i2}^{Q205L}$ and the GST-fusion C-terminal domain of TRPC4 was allowed to occur for 1 h at room temperature on a plate rotator. Each reaction sample was subsequently centrifuged at 500 × g for 5 min. After three washes with 500 μl PBS with 0.1% Triton X-100, the GST protein-G-protein complexes were eluted with 15 μl 2 × SDS sample buffer, and the entire sample was run on a 10% polyacrylamide-SDS gel. Mouse monoclonal anti-$G\alpha_{i2}$ (Santa Cruz, USA) and anti-GST antibodies (sc-138, Santa Cruz, USA)

were used for immunoblot analyses. Unless otherwise stated, all pull-down assays were repeated three times for each condition.

Whole-cell patch-clamp experiment

The whole-cell configuration was used to measure TRPC channel current in HEK cells as described previously (Kim et al, 2006; Lee et al, 2005; Jeon et al, 2008; Sung et al, 2011). Cells were transferred to a small chamber on the stage of an inverted microscope (TE2000S, Nikon, Japan), and attached to coverslips in the small chamber for 10 minutes prior to patch recording. Currents were recorded using an Axopatch 200B patch-clamp amplifier (Axon Instrument, USA). Bath solutions were constantly perfused with a physiological salt solution at a rate of 1-2 ml/min. Glass microelectrodes with 2-4 MΩ resistance were used to obtain gigaohm seals. After establishing the whole-cell configuration, the external solution was changed from Normal Tyrode to Cs^+-rich external solution. The current was recorded in 500 ms duration RAMPs from +100 to -100 mV and from a holding membrane potential of -60 mV. pCLAMP software v.10.2 and Digidata 1440A (Axon Instruments, USA) were used for data acquisition and application of command pulses. Data were filtered at 5 kHz and displayed on a computer monitor. Data were analyzed using pCLAMP v.10.2 and Microcal origin software v.7.5.

Solutions and Drugs

For all TRPC channel recordings, physiological salt solution (PSS) containing 135 mM NaCl, 5 mM KCl, 2 mM $CaCl_2$, 1 mM $MgCl_2$, 10 mM glucose, and

10 mM HEPES (*N*-[2-hydroxyethyl] piperazine-*N'*-[2-ethanesulphonic acid]). The pH was adjusted to 7.4 using NaOH. Cs^+-rich external solution was prepared by replacing NaCl and KCl with equimolar CsCl. The pipette solution contained 140 mM CsCl, 10 mM HEPES, 0.2 mM Tris-GTP (Tris-guanosine 5'-triphospate), 0.5 mM EGTA, and 3 mM Mg-ATP (Adenosine 5'-triphosphate). The pH was adjusted to 7.3 with CsOH. *Pertussis* toxin was purchased from Calbiochem (Germany), and carbachol, HEPES, and GTPγS were purchased from Sigma (USA).

Modeling of the interaction between $G\alpha_{i2}$ and TRPC4

The homology model of $G\alpha_{i2}$ structure was constructed using MODELLER 9v8 (Sali et al, 1993) based on two Gα structures that have high sequence homology with $G\alpha_{i2}$ (PDB id: 2ODE and1GP2). Due to the absence of a known protein structure homologous to TRPC4, the structure of TRPC4 C-terminus was modeled using I-TASSER, which combines the methods of threading, *ab initio* modeling and structural refinement (Roy et al, 2010; Zhang et al, 2008). The docking of the TRPC4 C-terminus on the $G\alpha_{i2}$ was initiated because the putative binding site of TRPC4 (amino acids 701-720) contains positive charges conserved among TRPC channels. An ionic interaction was assumed between the sites of the mTRPC4 and $G\alpha_{i2}$. There are 9 sites where the $G\alpha_i$ family has negative charges, but the $G\alpha_{q/11}$ family does not. Seven crystal structures of protein complexes between Gα and other proteins (PDB id: 2RGN, 2ODE, 3CX6, 2G83, 1FQJ, 2BCJ, and 1GP2) were visually inspected, and it was found that only specific areas of Gα participated in interactions with other proteins. Therefore, manual docking was carried out

between $G\alpha_{i2}$ and the TRPC4 C-terminus, emphasizing the close interaction between the two conserved positive charges of TRPC4, Arg711 and Lys715, and the conserved positive charges of $G\alpha_{i2}$, Asp252.

Statistics

All data are expressed as means ± SEM. Statistical significance was determined using paired or unpaired Student's *t*-tests. P values of less than 0.05 were considered statistically significant. The number of cell recordings is represented by *n*.

Results

Expression of TRPC4 alone results in a minimal spontaneous current (2.1 ± 1.1 pA/pF; Figure 3B mock, open column, n = 5), compared with TRPC5, which showed a significant basal current (Figure 3C, 36.6 ± 9.2 pA/pF, n = 14; see also ref. Sung et al, 2011). Although HEK cells endogenously express muscarinic receptors, most likely the M3 subtype (Miller et al, 2011), the endogenous receptors do not activate TRPC4 (Figure 1B mock and ref. Sung et al, 2009). In the case of TRPC5, the endogenous muscarinic receptor elicited only small transient TRPC5 activation. Therefore, we analyzed the TRPC4 and TRPC5 currents induced by heterologously expressed muscarinic receptors or by intracellular infusion of GTPγS through the patch pipette. The TRPC maximal inward currents (in Cs^+ rich solution) at negative membrane potentials (-60 mV) are represented as a current density (pA/pF). In all cases, maximal peak inward currents were obtained by subtracting the current recorded in bath Cs^+.

Endogenous $G\alpha_{i/o}$ activates TRPC4 and TRPC5 trough muscarinic receptor stimulation.

Firstly, we tested the effects of the expressed $G\alpha_i$-coupled M2 and the $G\alpha_q$-coupled M3 muscarinic receptors on the activation of TRPC4 or TRPC5 by endogenous G proteins in HEK cells (Figure 1 and 2). Activation of the M2 receptors with carbachol (CCh) elicited 2-3 fold higher TRPC4 and TRPC5 currents than activation of the M3 receptors. The TRPC4 and TRPC5 currents showed a typical doubly rectifying current-voltage relationship (Figure 1A

and 2A). The stimulation of the M2 receptor increased both TRPC4 and TRPC5 currents in a dose-dependent manner (Figure 1B & 2B, open column, 1 μM, 10 μM, 100 μM: n = 5, n = 4, n = 12 & n = 4, n = 4, n = 10), whereas the stimulation of the M3 receptor increased the TRPC4 current dose-dependently and the TRPC5 current dose-independently at the concentration range 1-100 μM μCCh (Figure 1B & 2B, closed column, 1 μM, 10 μM, 100 μM: n = 5, n = 8, n = 16 & n = 5, n = 7, n = 11). Treatment with PTX markedly inhibited the TRPC4 and TRPC5 currents activated by M2 receptor stimulation and GTPγS (Figure 1C, D & Figure 2C, D; Mock/PTX: n = 8/n = 8, n = 5/n = 5 & n = 7/n = 4, n = 6/n = 3). Thus, the M2R-$G\alpha_{i/o}$ pathway was more effective than the M3R-$G\alpha_q$ pathway in channel activation by engaging the endogenous PTX-sensitive Gα proteins.

Specific Gα isoforms increase TPRC4 and TRPC5 activity.

To determine which Gα isoform is involved in the activation of TRPC4 and TRPC5, we used constitutively active forms of the $G\alpha_i$ subunits (Gα QL mutants). Intracellular application of GTPγS through the patch pipette increased the TRPC4 current to 45.0 ± 7.2 pA/pF (Figure 3B mock, closed column, n = 13). The TRPC4 channel was activated to a different extent by all constitutively active $G\alpha_{i/o}$ subunits, even in the absence of GTPγS. Constitutively active $G\alpha_{i3}$ and $G\alpha_o$ mimicked the activation of TRPC4 by GTPγS (open/closed column, n = 10/n = 8 and n = 9/n = 11). Constitutively active $G\alpha_{i1}$ activated the TRPC4 channel, whereas application of GTPγS significantly inhibited the TRPC4 current (open/closed column, n = 13/n =

11). Constitutively active $G\alpha_{i2}$ ($G\alpha_{i2}^{Q205L}$) was the most effective activator among the $G\alpha_i$ subunits tested (Figure 3B open columns and Figure 4A, $n = 6$). Notably, the application of GTPγS had no further effect on the TRPC4 current, indicating that $G\alpha_{i2}$ fully activates TRPC4 (closed column, $n = 8$). Furthermore, stimulation of the M2 receptors (Figure 1) and $G\alpha_{i2}$ (Figure 3) activated TRPC4 to the same extent. Of particular significance, constitutively active $G\alpha_q$ was unable to activate TRPC4 (Figure 3B, open/closed column, $n = 4/n = 3$). Moreover, constitutively active $G\alpha_q$ inhibited the stimulatory effect of GTPγS. This is addressed further below.

Again, TRPC5 showed significant basal activity (36.6 ± 9.2 pA/pF, Figure 3C mock, open column). As with TRPC4, application of GTPγS further increased the TRPC5 current to 130.7 ± 16.7 pA/pF (Figure 3C mock, closed column, $n = 14$). $G\alpha_{i3}^{Q205L}$ was the most effective activator of TRPC5, as all other Gα isoforms tested actually reduced the spontaneous current and GTPγS-induced currents, likely by competing with endogenous $G\alpha_{i3}$ (Figure 3C & Figure 4B, open/closed column; $G\alpha_{i1}$, $G\alpha_{i2}$, $G\alpha_{i3}$, and $G\alpha_o$: $n = 12/n = 9$, $n = 6/n = 4$, $n = 7/n = 5$, and $n = 8/n = 9$). GTPγS did not increase the TRPC5 current activated by $G\alpha_{i3}^{Q205L}$. As was found with TRPC4, constitutively active $G\alpha_q$ was not able to activate TRPC5 and instead inhibited the TRPC5 current (open/closed column, $n = 3/n = 3$).

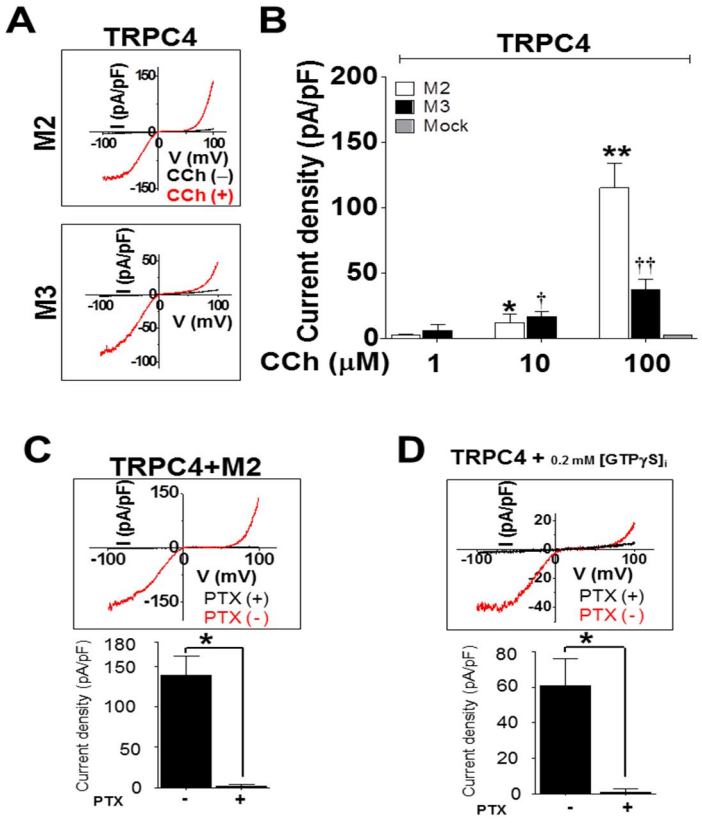

Figure 1. Activation of endogenous $G\alpha_{i/o}$ by the muscarinic M2 receptor activates TRPC4.

(A) CCh activated-TRPC4 current was recorded in HEK cells expressing TRPC4 and either M2 and M3 receptors. The representative *I-V* relationships of M2- and M3-evoked TRPC4 currents by 100 μM CCh were recorded by voltage RAMPS of +100 to -100 mV during 500 ms durations, while the cells were held at -60 mV. (B) Summarizes amplitude of M2- and M3-activated TRPC4 currents activated by 1-100 μM CCh. Current density is represented by maximal current peaks (subtracted Cs^+ basal current) at -60 mV in Cs^+ solution (changed from Normal Tyrode: Na^+) and is indicated by means ± S.E. Statistical significance was denoted by * (open column, 1 μM *vs* 10 μM) and ** (open column, 10 μM *vs* 100 μM), † (closed column, 1 μM *vs* 10 μM) and †† (closed column, 10 μM *vs* 10 μM) at $p < 0.05$. (C), (D) *I-V* relationship and current densities of M2- and GTPγS-evoked TRPC4 currents show inhibition by PTX pretreatment (100 ng/ml for 16 hr). Statistical significance was denoted by * ($p < 0.05$).

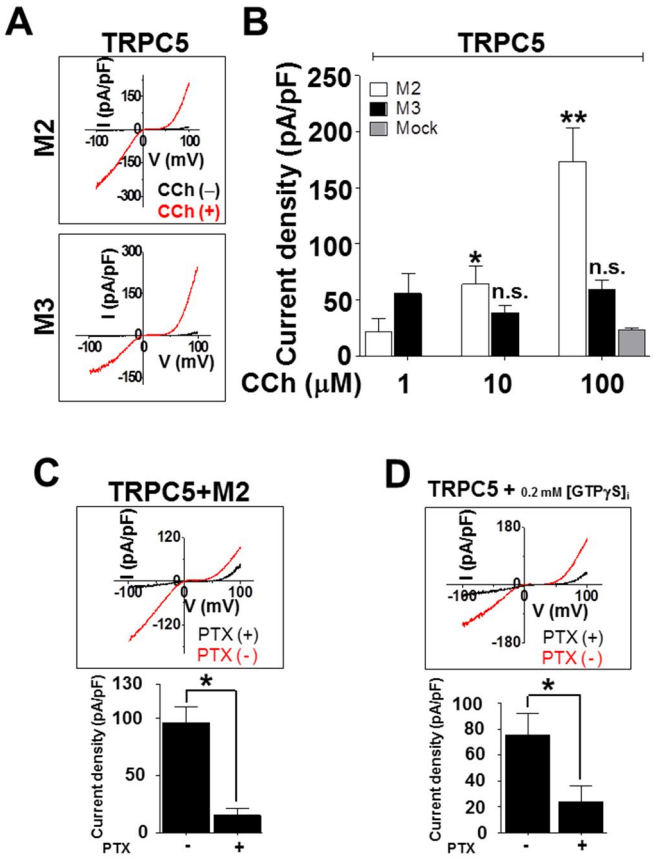

Figure 2. Activation of endogenous $G\alpha_{i/o}$ by the muscarinic M2 receptor activates TRPC5.

(A) The representative *I-V* relationships of M2- and M3-activated TRPC5 currents were measured in cells stimulated with 100 μM CCh. (B) Summary of the M2-activated TRPC5 current at 1-100 μM CCh. Current density was obtained by the methods described above. Statistical significance was denoted by * (open column, 1 μM *vs* 10 μM) and ** (open column, 10 μM *vs* 100 μM) at $p < 0.05$. (C), (D) The representative *I-V* relationships and current densities of M2- and GTPγS-evoked TRPC5 currents show inhibition by PTX pretreatment (experimental procedure described above). Statistical significance was denoted by * ($p < 0.05$).

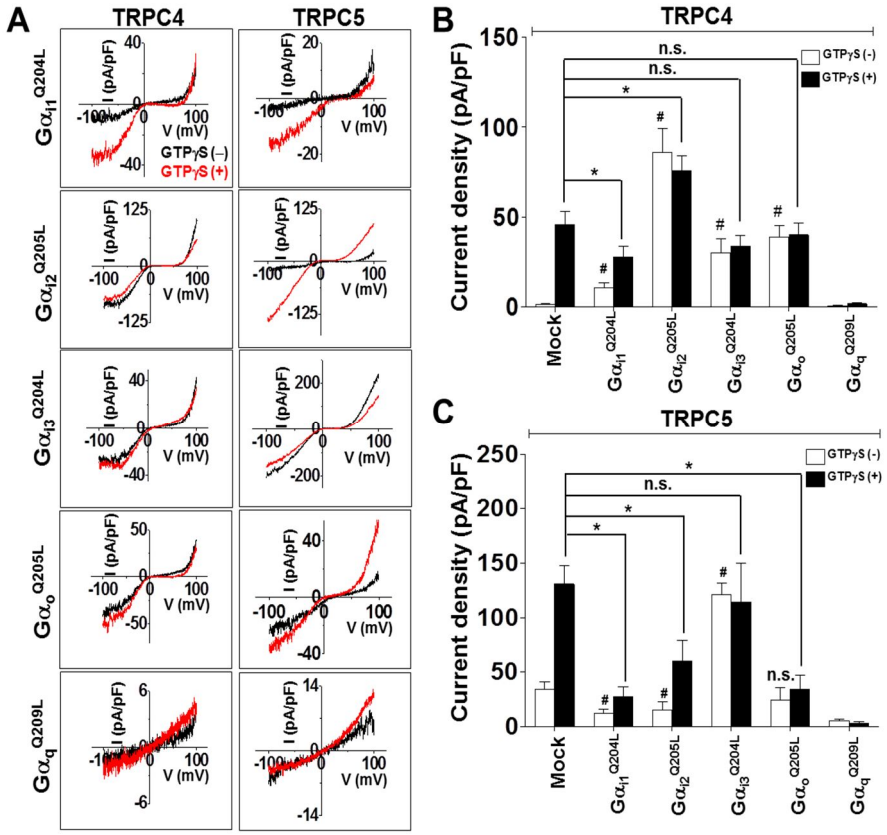

Figure 3. Effect of Gα isoforms on TPRC4 and TRPC5 activity.
(A) Representative *I-V* relationships of TRPC4 and TRPC5 show the effect of constitutively active Gα QL mutants on the electrophysiological properties of the TRPC4 and TRPC5 channels. (B) Summary of TRPC4 current density activation by Gα subunits and/or by GTPγS. Note the variable effects of the Gα mutants. All Gα mutants activate TRPC4 channels without an activator (e.g. GTPγS or CCh). $G\alpha_{i2}$ provided the most effective activation of TRPC4, whereas $G\alpha_q$ inhibited TRPC4. Current density is represented by maximal current peaks (subtracted Cs^+ basal current) at -60 mV in Cs^+ solution and is indicated by means ± S.E. Statistical significance was denoted by * (closed column) and # (open column) at $p < 0.05$. (C) Summary of TRPC5 activation by Gα subtypes showing that the most effective activator is $G\alpha_{i3}$ and that most Gα mutants inhibit the TRPC5 channel, with $G\alpha_q$ inhibiting TRPC5. Current density was obtained by the methods described above. Statistical significance was denoted by * (closed column) and # (open column) at $p <$ 0.05.

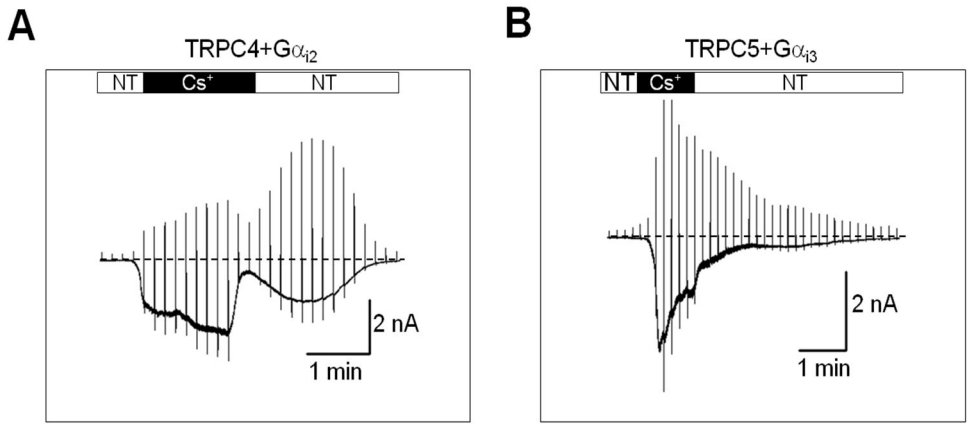

Figure 4. Recording of the $G\alpha_{i2}$-activated TRPC4 and of the $G\alpha_{i3}$-activated TRPC5 currents.
(A) Representative current trace of TRPC4 co-expressed with $G\alpha_{i2}$ showing that $G\alpha_{i2}$ activates the TRPC4 current. (B) Representative current trace of TRPC5 co-expressed with $G\alpha_{i3}$ showing that $G\alpha_{i3}$ activates TRPC5. Both current traces are recorded at -60 mV in external solution changed from NT (Normal tyrode: Na^+) to Cs^+ solution. The *horizontal bar* indicates duration of applied external cation solutions from both traces. *Dashed lines* show zero current.

Gβγ isoforms are not required for TPRC4 and TRPC5 activation.

While $G\alpha_{i/o}$ subunits are key activators of TRPC4 or TRPC5, Gβγ subunits may also be involved in the activation of the channels, as is the case with GIRK channels or in the regulation of the channels by altering the availability of activated $G\alpha_i$. To address these questions, we tested the effects of various Gβγ combinations on TRPC4 and TRPC5 activity. Figs. 5A-C show that none of the Gβγ combinations tested activated the channels or reduced the activation by GTPγS. The exception is $G\beta_2\gamma_2$, which slightly inhibited the activation of TRPC5, likely by sequestering some of the $G\alpha_{i3}$ even in the presence of GTPγS. Moreover, even the free form $G\beta_1^{I80A}$ mutant (Ford et al, 1998; Riven et al, 2006) did not activate TRPC4 or TRPC5 (Figure 5B; open/closed column n = 4/ n = 5, 3C; open/closed column n = 3/ n = 14). These results indicate that the PTX-sensitive $G\alpha_{i2/3}$ subunits are the activators of TRPC4 and TRPC5.

As is shown with the use of the Gβ mutant, $G\beta_1^{W99A}$, the major role of $G\beta_2\gamma_2$ in the activation of TRPC4 and TRPC5 is the sequestering of $G\alpha_{i/o}$ subunits. $G\beta_1^{W99A}$ keeps the G protein as the heterotrimer Gαβγ because $G\beta_1^{W99A}$ is unable to support nucleotide exchange on Gα (Riven et al, 2006). $G\beta_1^{W99A}$ inhibited activation of TRPC4 by M2 receptor stimulation to 61.4% ± 7.0% (p = 0.03, without/with $G\beta_1^{W99A}$ n = 10/n = 12), whereas $G\beta_1^{W99A}$ did not inhibit the modest M3-induced TRPC4 current (without/with $G\beta_1^{W99A}$: n = 8/n = 10). With TRPC5, $G\beta_1^{W99A}$ inhibited M2-induced TRPC5 current to 53.4% ± 16.7% (p = 0.02, without/with $G\beta_1^{W99A}$: n = 11/n = 8), without affecting the minimal M3-induced TRPC5 current (without/with $G\beta_1^{W99A}$: n = 4/n = 6,

Figure 6A). Importantly, $G\beta_1^{W99A}$ inhibited GTPγS-induced TRPC4 current to 46.2% ± 4.4% (p = 0.00079, without/with GTPγS: *n* = 9/*n* = 8) and GTPγS-induced TRPC5 current to 28.7% ± 7.7% (p= 0.00075, without/with GTPγS: *n* = 6/*n* = 6, Fig. 6B).

TRPC4 is inhibited by increased $G\alpha_q$ activity.

Activation of the $G\alpha_q$-PLC pathway has been shown to modestly activate TRPC4 and TRPC5 (Schaefer et al, 2000; Kim et al, 2008; Otsuguro et al, 2008, and Figure 1) by an unknown mechanism. Hence, the inhibition of TRPC4/5 by the constitutively active $G\alpha_q$ (Figure 3) was completely unexpected. These results imply that intense overstimulation of a $G\alpha_q$-activated pathway inhibits TRPC4 and TRPC5. We considered several potential mechanisms, including increased or decreased cytoplasmic Ca^{2+}, interference of channel interaction with $G\alpha_i$, reduced surface expression of TRPC4, modified cellular PIP_2 and channel phosphorylation by PKC, known to induce desensitization of TRPC5 with phosphorylation of residue T972 at the C-terminus (Zhu et al, 2005).

Loading the cells with BAPTA-AM recovered only 15 ± 5.6% (mock: 56.7 ± 11.2 pA/pF; *n* = 6, recovery by BAPTA: 9.8 ± 3.1 pA/pF; *n* = 6, BAPTA with GTPγS; *n* = 12, $G\alpha_q$ QL; *n* = 3, Figure 7A), and inhibition of PKC with Goe6976 recovered only 13 ± 8.7% (mock: 67.6 ± 12.6 pA/pF; *n* = 5, recovery by PKC inhibitor: 10.1 ± 5.8 pA/pF; *n* = 8, $G\alpha_q$ QL; *n* = 3, Figure 7B) of the TRPC4 current inhibited by $G\alpha_q$. The $G\alpha_q$-TRPC4 inhibited current was recovered to only 27.7 ± 9.2% by 5 μM intracellular Ca^{2+} (without $G\alpha_q^{Q209L}$: non-buffered/5 μM, *n* = 7/ *n* = 3, with $G\alpha_q^{Q209L}$: non-buffered/5 μM, *n* = 3/ *n* =

3; Figure 7C). Co-IP experiments showed that TRPC4 does not interact directly with $G\alpha_q$ (Figure 7D). Finally, activated $G\alpha_q$ did not change the surface expression of TRPC4 (Figure 7F, upper blots). These findings rule out the effects of changes in cytosolic Ca^{2+}, PKC, and altered interaction with $G\alpha_i$ in channel inhibition by $G\alpha_q$ as the major inhibitors of the current induced by activated $G\alpha_q$. Moreover, they point to an indirect effect of $G\alpha_q$ on channel function.

$G\alpha_q$ activates PLC to hydrolyze PIP_2, reported to have an effect of TRPC4 and TRPC5 channel activity (Kim et al, 2008; Otsuguro et al, 2008). When diC8-PIP2 (50 μM) was applied via the patch pipette together with GTPγS, it recovered $G\alpha_q$-induced inhibition of TRPC4 up to 51.83 ± 12.83% of the PIP_2 control (open/closed column, mock, PIP_2 alone, $G\alpha_q^{Q209L}$, and PIP_2 with $G\alpha_q^{Q209L}$; n = 18/26, n = 4/15, n = 3/18, and n = 3/14, Figure 7E). PIP_2 was reported to inhibit TRPC4α but not the TRPC4β isoform (Otsuguro et al, 2008), the isoform used in the present work. In addition, we reported that PIP_2 slows TRPC5 desensitization (Kim et al, 2008). Thus, the combined results in Fig. 4 indicate that PIP_2 and perhaps increased cytoplasmic Ca^{2+} are required for TRPC4 and TRPC5 activation.

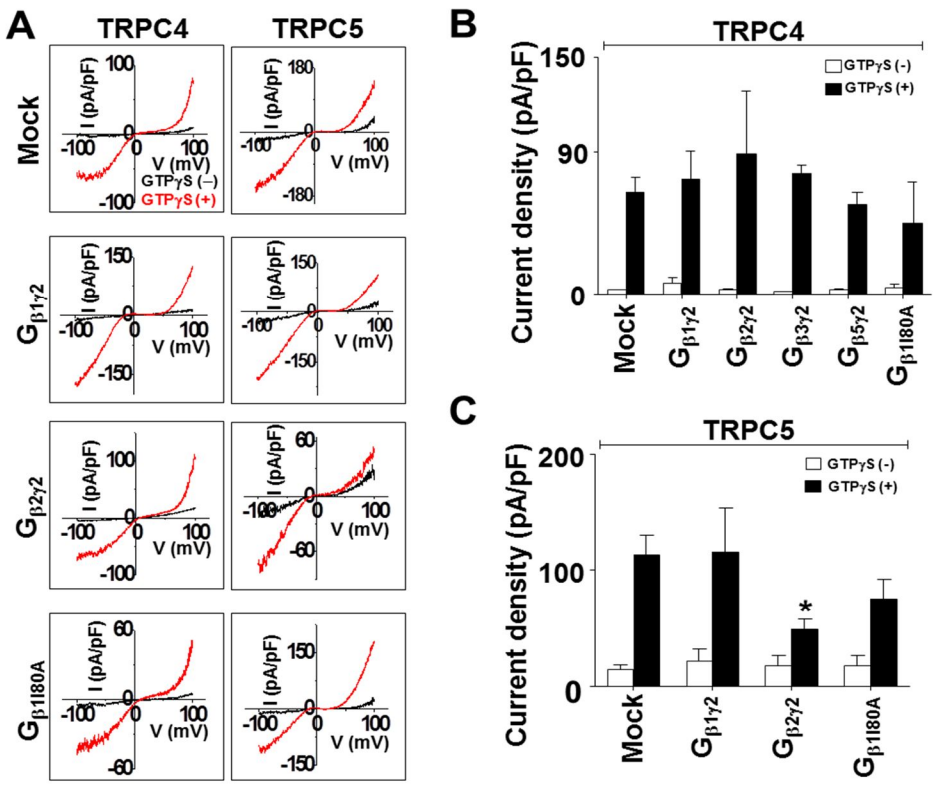

Figure 5. Lack of effect of Gβγ isoforms on TPRC4 and TRPC5 activity. Panel (A) shows representative *I-V* curves of TRPC4 and TRPC5 co-expressed with or without the indicated Gβγ isoforms. Panels (B) and (C) summarize the current density recorded in cells transfected with the indicated Gβγ subunits and infused with GTPγS (closed columns; mock, $G\beta_1\gamma_2$, $G\beta_2\gamma_2$, $G\beta_3\gamma_2$, and $G\beta_5\gamma_2$ with TRPC4: $n = 24$, $n = 5$, $n = 3$, $n = 7$, and $n = 7$; mock, $G\beta_1\gamma_2$, and $G\beta_2\gamma_2$ with TRPC5: $n = 10$, $n = 8$, and $n = 6$) or without (open columns; mock, $G\beta_1\gamma_2$, $G\beta_2\gamma_2$, $G\beta_3\gamma_2$, and $G\beta_5\gamma_2$ with TRPC4: $n = 15$, $n = 5$, $n = 4$, $n = 5$, and $n = 4$; mock, $G\beta_1\gamma_2$, and $G\beta_2\gamma_2$ with TRPC5: $n = 3$, $n = 5$, and $n = 3$). All current densities represent maximal current peaks (subtracted Cs^+ basal current) at -60 mV in Cs^+ solution and are indicated by means ± S.E. Statistical significance was denoted by * ($p < 0.05$).

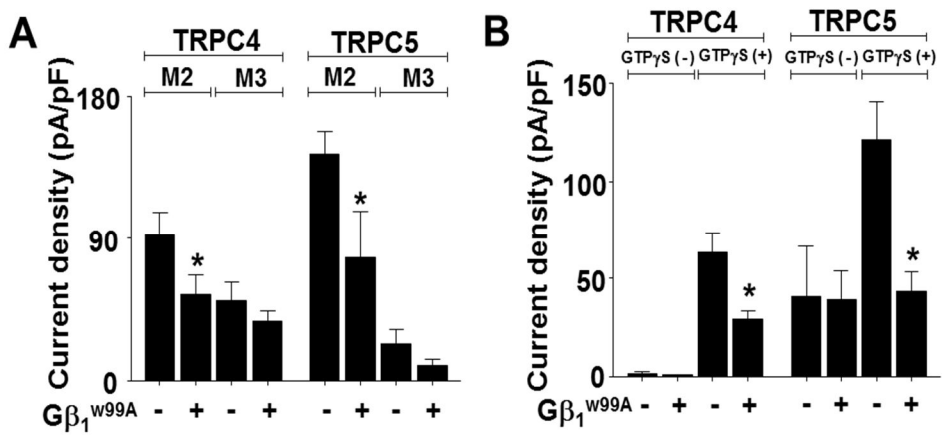

Figure 6. Effect of $G\beta_1^{W99A}$ isoforms on TPRC4 and TRPC5 activity.
Panel (A) shows the effects of $G\beta_1^{W99A}$ on activation of TRPC4 and TRPC5 by muscarinic receptors. The activation of TRPC4 and TRPC5 by the M2 receptor was inhibited by $G\beta_1^{W99A}$, while no current was activated by the M3 receptors. (B) Inhibition by $G\beta_1^{W99A}$ of TRPC4 and TRPC5 activated by GTPγS. All current densities represent maximal current peaks (subtracted Cs^+ basal current) at -60 mV in Cs^+ solution and are indicated by means ± S.E. Statistical significance was denoted by * ($p < 0.05$).

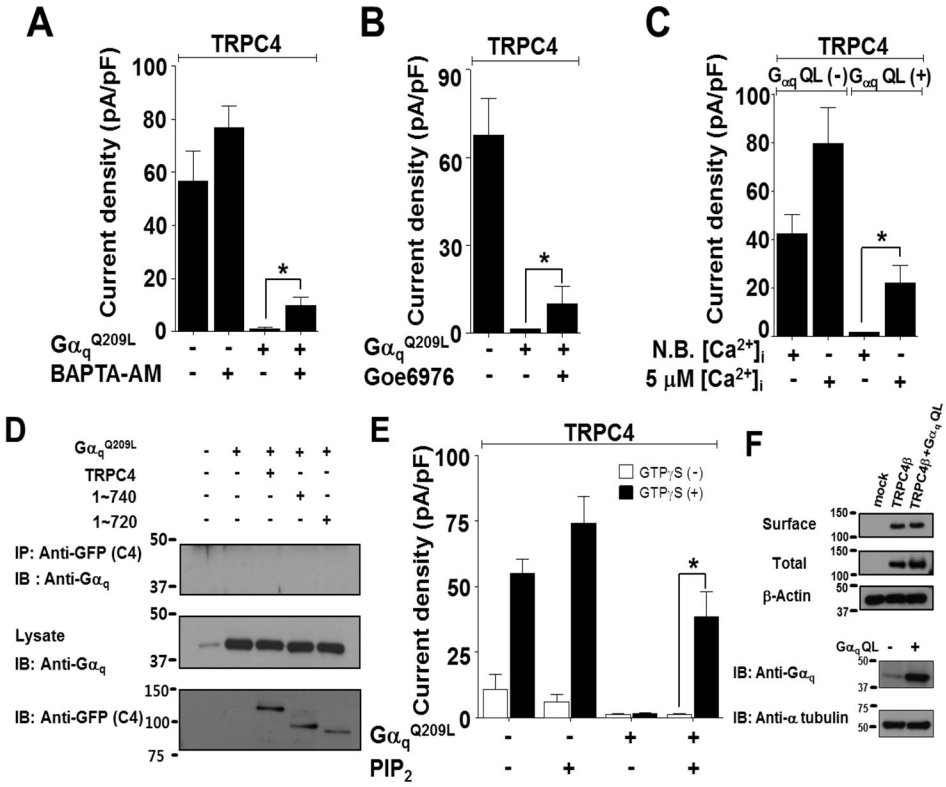

Figure 7. Inhibition of TRPC4 by $G\alpha_q$ is rescued by PIP2.
Panels (A)-(C) show current densities in HEK293 cells stably expressing mTRPC4 and its inhibition by $G\alpha_q$. Loading the cells with BAPTA-AM and inhibition of PKC with Goe6976 did not effectively reverse channel inhibition by $G\alpha_q$. High intracellular Ca^{2+} (5 μM) reversed channel inhibition by $G\alpha_q$. (D) TRPC4 and C-terminal truncation TRPC4 mutants did not co-IP with $G\alpha_q$. (E) Intracellular application of diC8-PIP_2 (50 μM) almost recovered the inhibition of TRPC4 by $G\alpha_q$. All current densities represent subtracted-maximal current peaks at -60 mV in Cs^+ solution and are indicated by means ± S.E. Statistical significance was denoted by * ($p < 0.05$). All whole-cell currents were recorded in the intracellular application of GTPγS. (F) Surface expression of TRPC4 and $G\alpha_q$ co-expressed TRPC4 in HEK cells. Surface expression of TRPC4 was not altered by $G\alpha_q$ QL as determined by co-expression and surface biotinylation. Immunoblots of surface and total were detected by anti-GFP antibody (upper panel). Expression of endogenous $G\alpha_q$ and transfected $G\alpha_q$ QL were detected by $G\alpha_q$ antibody (bottom panel).

Mechanisms associated with the interaction between $G\alpha_{i2}$ with the C-terminus of TRPC4.

Together, the results in Figs. 1-7 indicate that activation of $G\alpha_i$ subunits by GPCRs is the primary mechanism for activating TRPC4 and TRPC5. This raised the question of whether activation of the channels requires direct interaction with the $G\alpha_i$ subunits, as was shown for other channels regulated by Gα (Clancy et al, 2005) and Gβγ (Ford et al, 1998; Finley et al, 2004) subunits. To address this question, we identified the TRPC4 and TRPC5 domain that might interact with the $G\alpha_i$ subunits. To characterize the association between TRPC4β with $G\alpha_{i2}$ *in vivo*, HEK cells were transfected with TRPC4β-GFP and $G\alpha_{i2}$, and their association was analyzed by co-immunoprecipitation. Immunoprecipitation of $G\alpha_{i2}$ pulled down TRPC4β-GFP (Figure 8A upper panel). Likewise, $G\alpha_{i2}$ was present in TRPC4β-GFP immunoprecipitates (Figure 8A lower panel). Similar co-immunoprecipitation occurred between TRPC5 and $G\alpha_{i3}$ (Figure 9A). Pull-down assays were utilized to examine the binding of purified $G\alpha_{i2}^{Q205L}$ to GST fusion protein containing the C-terminal domain of TRPC4. $G\alpha_{i2}^{Q205L}$ bound to the C-terminal domain of TRPC4 (Figure 8A right panel).

To map the $G\alpha_{i2}$ binding domain in TRPC4β, a series of TRPC4β-GFP truncation or deletion mutants were generated (Figure 8B). Binding domains for regulatory molecules are clustered in the C-terminal region of TRPC4 and TRPC5. Because considerable evidence suggests that modulation of TRPC4 and TRPC5 function are directed by elements present in this region, we focused on the C-terminal region. We made deletion mutants based on well-known binding domains: the Calmodulin and IP_3 receptors binding region

(CIRB) (amino acids 695-724), the SEC14-like and spectrin-type domains 1 (SESTD1) (amino acids 700-728), and the α-spectrin binding domain (amino acids 730-758). Of the truncations shown in Figure 5C, Δ759-870 and Δ730-758 retained activation by $G\alpha_{i2}^{Q205L}$ with peak current amplitude similar to that of WT-TRPC4, although TRPC4 (Δ730-758) lost activation by GTPγS (open/closed column, mock, Δ695-724, Δ700-728, Δ730-758, and Δ759-870; *n* = 8/7, *n* = 3/5, *n* = 3/4, and *n* = 9/6; Figure 8C). These results implicate amino acids upstream of 730 in channel activation by $G\alpha_i$. To further narrow the functional site, we examined the function of the 11 deletion or truncation TRPC4 mutants listed in Figure 10A. $G\alpha_{i2}^{Q205L}$ did not activate TRPC4β-GFP 1-700, Δ700-710, Δ710-720, Δ700-740, Δ700-870, and Δ720-870, but fully or partially activated the other mutants with the typical doubly rectifying *I-V* curve (open/closed column, mock, Δ700-710, Δ710-720, Δ700-740, Δ720-730, Δ720-740, Δ720-870, Δ700-870, 1-760, 1-740, 1-720, and 1-700; *n* = 27/12, *n* = 3/4, *n* = 3/3, *n* = 3/3, *n* = 10/10, *n* = 9/7, *n* = 3/5, *n* = 3/3, *n* = 8/9, *n* = 10/6, *n* = 5/8, and *n* = 3/4; Figure 10B and Figure 11). Similarly, $G\alpha_{i3}^{Q205L}$ did not activate TRPC5-GFP Δ701-733, Δ707-717, Δ707-727, Δ707-735, Δ707-747, and Δ707-954, but fully or partially activated Δ737-765 and Δ764-954 (open/closed column, mock, Δ701-733, Δ707-747, Δ707-954, Δ737-765, and Δ764-954; *n* = 12/12 , *n* = 3/5, *n* = 3/3, *n* = 3/3, *n* = 3/3, *n* = 7/3, *n* = 3/3, *n* = 3/13, and *n* = 11/7; Figure 9).

The TRPC4β-GFP constructs were also co-expressed with $G\alpha_{i2}$ in HEK cells, and their interaction was monitored by co-immunoprecipitation. C-terminal (TRPC4β 1-720 and 1-740) truncations and TRPC4 (Δ721~740 and Δ759~870) deletions did not affect binding to $G\alpha_{i2}$, while deletion of the

SESTD1 binding domain (Δ700~728) or of Δ700~870 eliminated association with $G\alpha_{i2}$ (Figure 10C). Thus, the $G\alpha_{i2}$ binding domain maps to amino acids 700~728, the SESTD1 domain of TRPC4β.

To further analyze the interaction between the TRPC4 C-terminus and $G\alpha_i$, we prepared C-terminal fragments of TRPC4 and examined their interactions with $G\alpha_i$. TRPC4β (621–700) did not interact with $G\alpha_i$, but TRPC4 fragments 621-720, 621-740, and 621-760 did (Figure 10D), strengthening the conclusion that TRPC4 (701-720) mediates the interaction with $G\alpha_{i2}$. The TRPC4 (701-720) encompass the CaM and IR3R CIRB binding region (Tang et al, 2001; Figure 12). The modeling in Figure 13A of the interaction between $G\alpha_{i2}$ and TRPC4 suggested that the ^{711}RNLVKR^{716} region is important for binding, and thus, we prepared the mutants R711A, N712R, K715A, and R716A (Figure 13 and Figure 14). Of these mutants, K715A and R716A retained activation by $G\alpha_{i2}^{Q205L}$ with peak current amplitude similar to that of WT-TRPC4, while R711A and N712R lost partial or complete activation by both $G\alpha_{i2}^{Q205L}$ and GTPγS. However, the double mutant K715A/R716A did not respond to $G\alpha_{i2}^{Q205L}$ but maintained responsivity to GTPγS (open/closed column, mock, R711K, R711A, N712R, K715A, R716A, and K715A/ R716A; n = 6/11, n = 3/3, n = 15/3, n = 3/3, n = 3/9, n = 7/8, and n = 6/6, Figure 13B). These results implicate amino acids K715 and R716 in channel activation by $G\alpha_i$. Ordaz et al. (Ordaz et al, 2005) showed that a similar sequence in mTRPC5 (^{718}RNLVKR^{723}) is involved in the activation process by calmodulin (Ordaz et al, 2005). Thus, we used the mTRPC5 CIRBm1 (R718A/K722A/R723A), CIRBm2 (I717D/L720E/V721 A), and CBII mutants (ΔP828~N854) (Ordaz et al, 2005) to test properties of TRPC5

activation by $G\alpha_{i3}$ (open/closed column, mock, CIRBm1, CIRBm2, and CBII: n = 7/6, n = 4/6, n = 4/5, and n = 4/3 in absence of $G\alpha_{i3}$; Figure 15). The constitutively active $G\alpha_{i3}$ mutant could not activate the CIRBm1 and CIRBm2 deletion mutants but did activate the CBII mutant (open/closed column, mock, CIRBm1, CIRBm2, and CBII: n = 6/6, n = 5/3, n = 4/4, and n = 6/4; Figure 15). Interaction between $G\alpha_i$ and the TRPC channels can also be demonstrated *in vivo*, as revealed by co-IP of TRPC4 with $G\alpha_{i2}$ and of TRPC5 with $G\alpha_{i3}$ in brain extract (Figure 16).

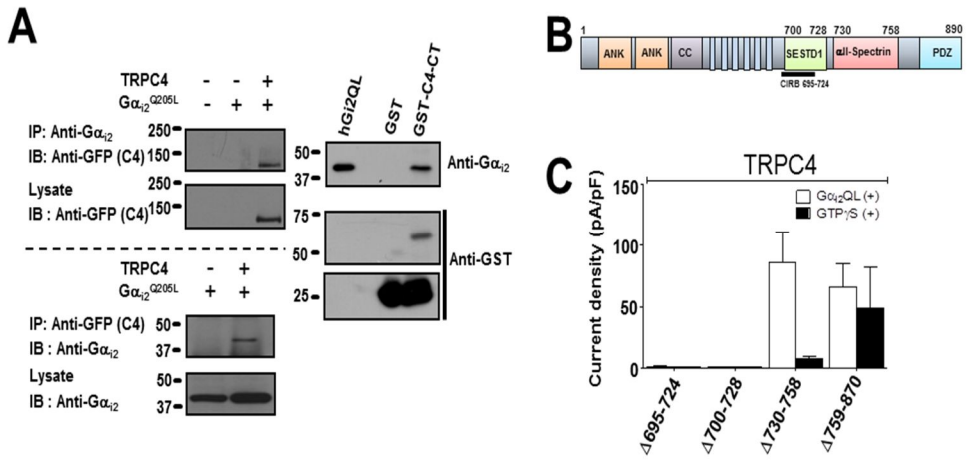

Figure 8. Association of $G\alpha_{i2}$ with TRPC4.

(A) TRPC4 co-immunoprecipitates with $G\alpha_{i2}$. HEK cells were transfected with empty vector, $G\alpha_{i2}$ alone, and $G\alpha_{i2}$ with TRPC4-GFP and were used to test reciprocal co-IP of TRPC4 and $G\alpha_{i2}$. TRPC4 C-terminal GST fusion protein was used to probe direct binding between $G\alpha_{i2}$ and TRPC4. Binding of the TRPC4 C-terminal GST fusion protein with recombinant human $G\alpha_{i2}^{Q205L}$ protein was shown by $G\alpha_{i2}$-antibody *in vitro* binding assay. (B) A schematic of GFP-fused TRPC4. (C) Summary of the effects of $G\alpha_{i2}$ on TRPC4 C-terminal truncation mutants in the presence and absence of GTPγS stimulation. Current densities are represented by subtracted-maximal maximal current peaks at -60 mV in Cs^{+} solution and are indicated by means ± S.E..

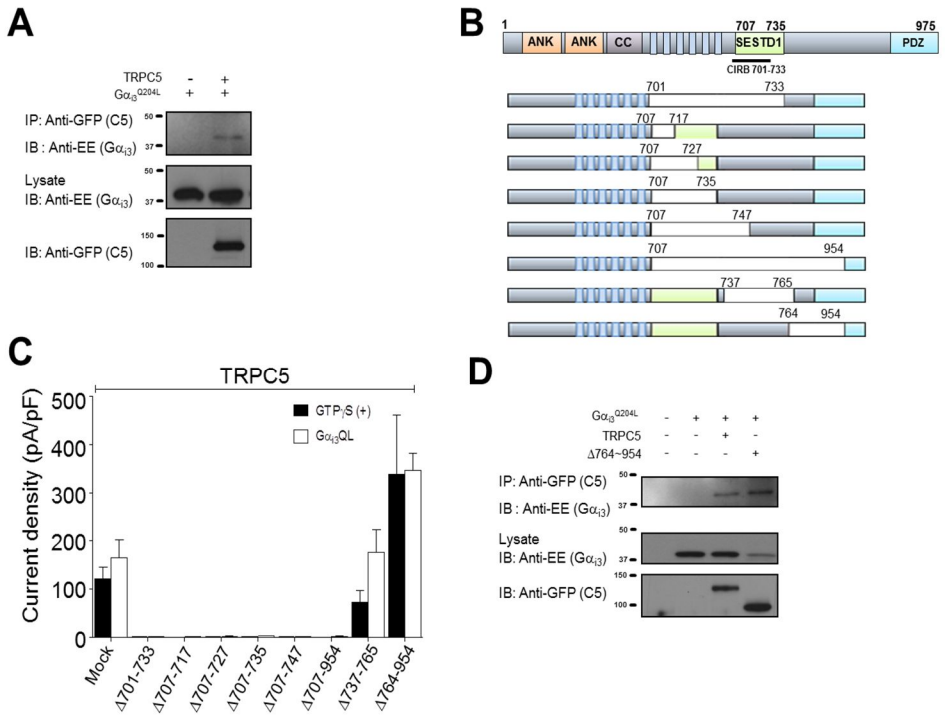

Figure 9. Interaction of $G\alpha_{i3}$ with the C-terminus of TRPC5.
(A) TRPC5 co-immunoprecipitates with $G\alpha_{i3}$. HEK cells were transfected with $G\alpha_{i3}$ alone or $G\alpha_{i3}$ with TRPC5-GFP and were used to test co-IP of TRPC5 and $G\alpha_{i3}$. TRPC5-GFP immunoprecipitated by GFP antibody and $G\alpha_{i3}^{Q205L}$ (containing internal epitope of EE) and was stained by EE-epitope antibody. (B) A schematic of GFP-fused mTRPC5 and mTRPC5 deletion mutants. (C) Summary of the effects of $G\alpha_{i3}^{Q205L}$ on current by TRPC5 deletion mutants in the presence and absence of GTPγS stimulation. Current densities are represented by maximal current peaks (subtracted Cs^+ basal current) at -60 mV in Cs^+ solution and are indicated by means ± S.E. (D) TRPC5 (764-954) is not required for interaction with $G\alpha_{i3}$.

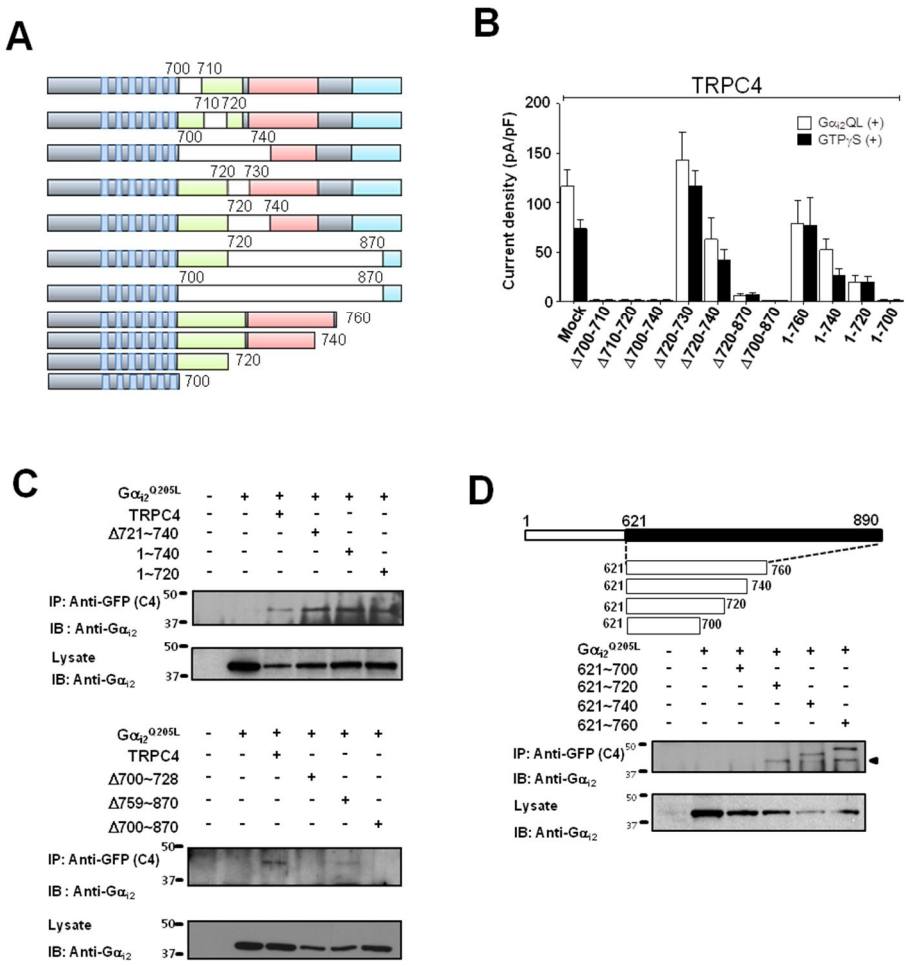

Figure 10. Interaction of $G\alpha_{i2}$ with the C-terminal region of TRPC4.
(A) Schematic of GFP-fused TRPC4 deletion and truncation mutants used (upper). Wild-type TRPC4 and mutants were probed using the GFP antibody in immunoblotting (bottom). (B) Summary of the effects of $G\alpha_{i2}$ on current by TRPC4 deletion and truncation mutants in the presence and absence of GTPγS stimulation. Current density was obtained by the methods described above. (C) Interaction between $G\alpha_{i2}$, TRPC4 and mutants was tested by co-IP, and the interaction site was mapped to the 700~728 region (the SESTD1 domain of TRPC4).

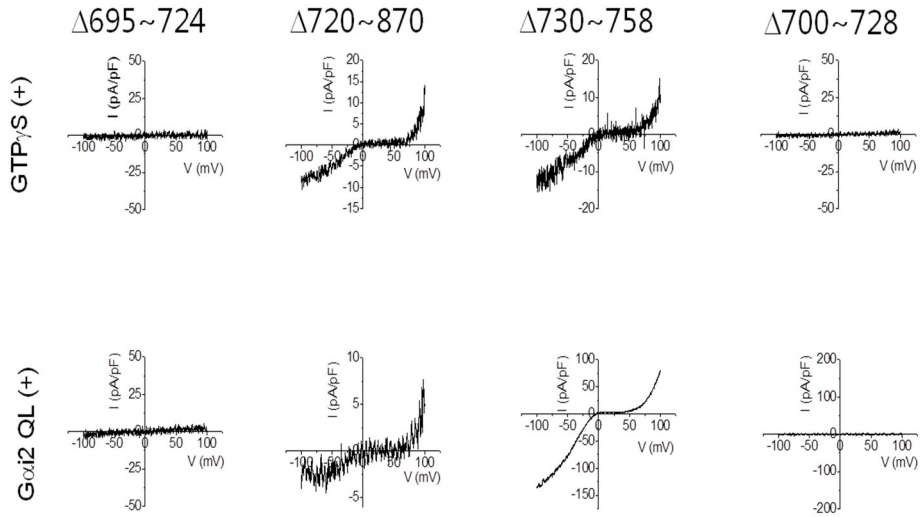

Figure 11. *I-V* curves of TRPC4 deletion mutants activated by GTPγS or $G\alpha_{i2}$.
The Δ695~724 and Δ700~728 mutants are not active, whereas the others retained partial or full activation.

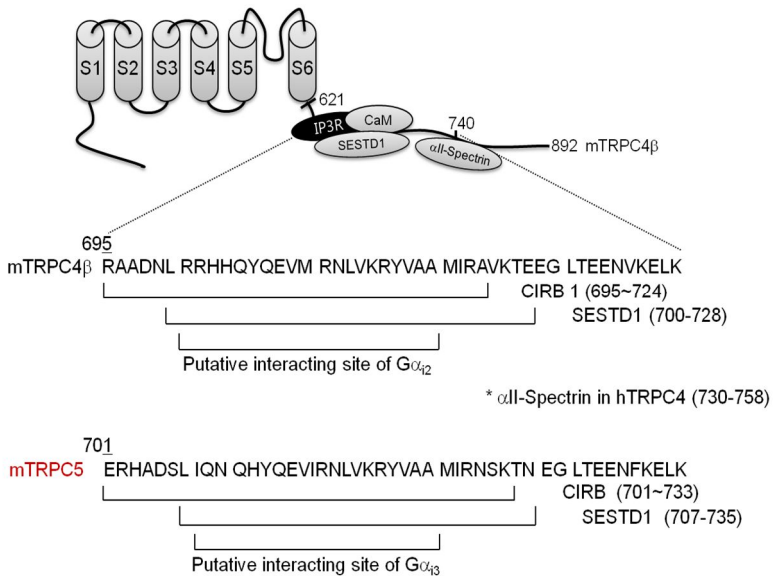

Figure 12. A schematic diagram of mTRPC4β and mTRPC5 depicting their Gα interacting sites.

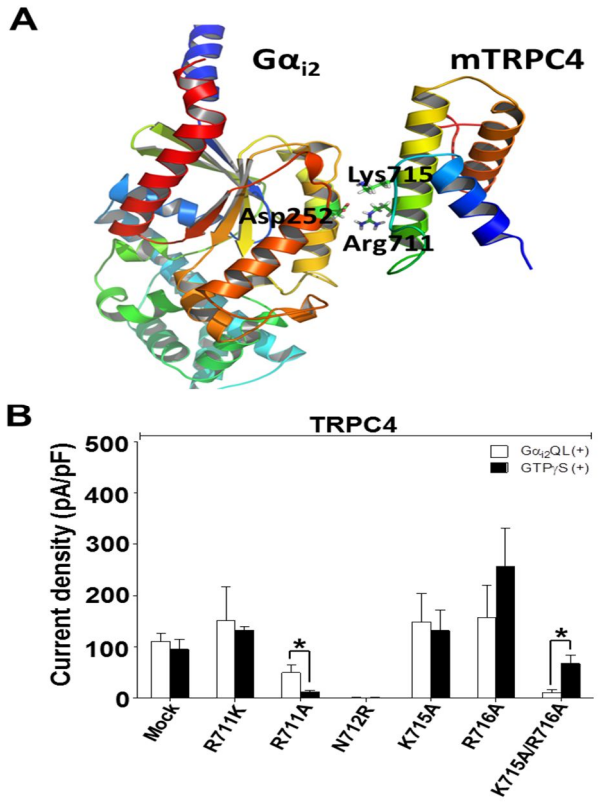

Figure 13. The interaction modeling of the TRPC4 C-terminus (amino acids 701 - 720) with $G\alpha_{i2}$.

(A) A model of association between $G\alpha_{i2}$ and TRPC4. An ionic interaction was assumed between the two proteins. Amino acids from 671 to 758 of TRPC4 are shown. (B) Summary of effects of $G\alpha_{i2}^{Q205L}$ on current by mTRPC4 and mTRPC4 mutants in the presence and absence of GTPγS stimulation. mTRPC4 mutants were substituted at CIRB residues (R711K, R711A, N712R, K715A, and R716A). All current densities represent maximal current peaks (subtracted Cs^+ basal current) at -60 mV in Cs^+ solution and are indicated by means ± S.E. Statistical significance was denoted by * ($p < 0.05$).

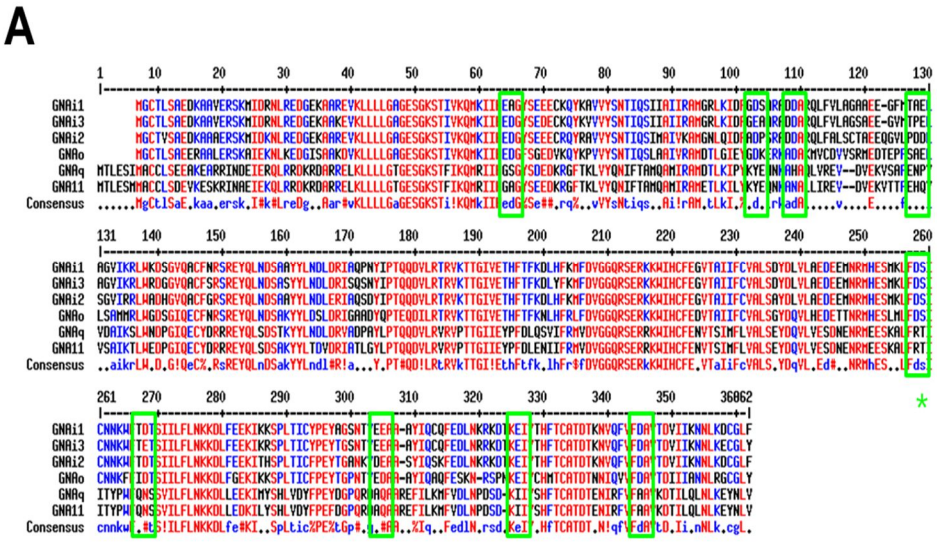

Figure 14. The Alignment of $G\alpha_{i/o}$ and $G\alpha_{q/11}$.
(A) Alignment of $G\alpha_i$ and $G\alpha_{q/11}$. Nine sites where the $G\alpha_i$ family has negative charges but the $G\alpha_{q/11}$ family does not are boxed in green. Among the nine sites of $G\alpha_{i2}$, only Asp252 belongs to areas of interaction with other proteins.

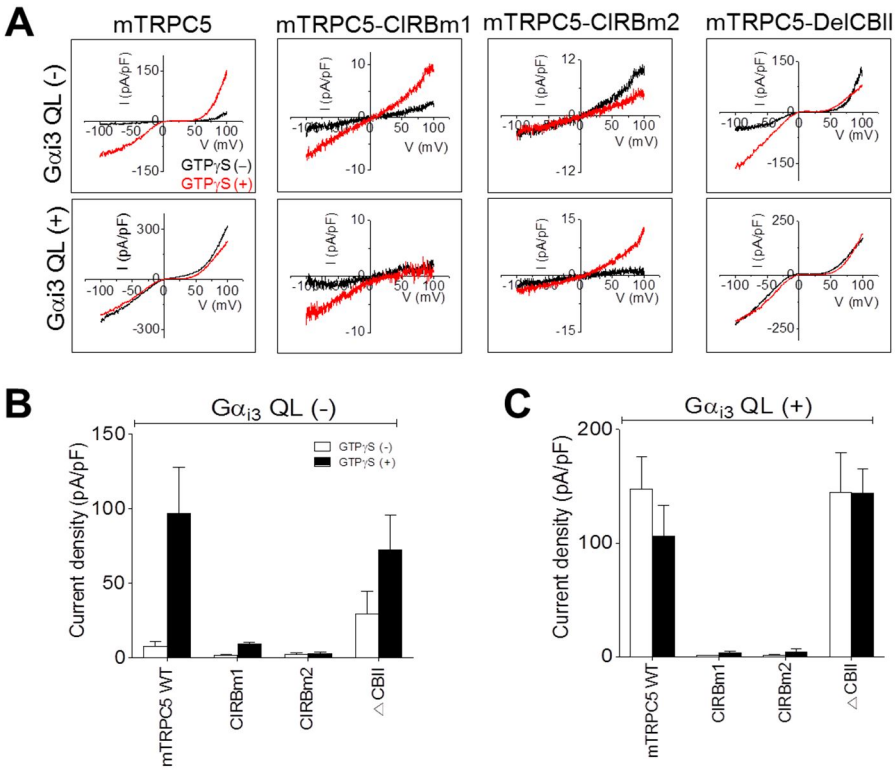

Figure 15. The CIRB region of TRPC5 is critical for channel activation by $G\alpha_{i3}$.

(A) Representative *I-V* curves of mTRPC5 currents with and without $G\alpha_{i3}^{Q205L}$. The black lines indicate the absence of GTPγS, and the red lines indicate activation by GTPγS infusion in patch pipette. Panels (B, C) Summary of the effects of $G\alpha_{i3}^{Q205L}$ on current by mTRPC5 and mTRPC5 deletion mutants in the presence and absence of GTPγS stimulation. The mTRPC5 CIRBm1 mutant was changed by substituting Arg718, Lys722, and Arg723 with alanine. Another mutant (CIRBm2) was substituted at CIRB residues (I717D/L720E/V721A). The CBII mutant is formed by deleting Pro828 to Asn854. All current densities are represented by maximal current peaks at -60 mV in Cs^+ solution and are indicated by means ± S.E.

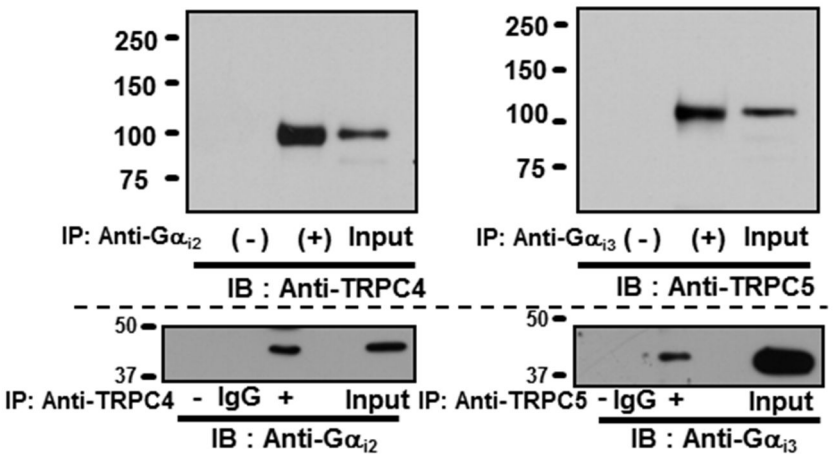

Figure 16. Interaction of $G\alpha_{i2}$ with TRPC4 and $G\alpha_{i3}$ with TRPC5 in brain extract.

(A) A schematic of GFP-fused C-terminal fragments of TRPC4 (upper) and their co-IP with $G\alpha_{i2}$. (H) The association between $G\alpha_i$ with TRPC4/5 *in vivo*. $G\alpha_{i2}$ and $G\alpha_{i3}$ were immunoprecipitated from rat brain extract and were probed for TRPC4 and TRPC5 to show co-IP *in vivo* (upper). TRPC4 and TRPC5 were co-immuno precipitated reciprocally. Lanes of IgG and control (-) did not show $G\alpha_i$ binding. Input was indicated as 10% input of brain extract

Discussion

We report here that the primary mechanism for the activation of TRPC4 and TRPC5 in gastric smooth muscle *in vivo* is through activation of GPCR. TRPC4 and TRPC5 activation appears to require both M2-$G_{i/o}$ and M3-$G_{q/11}$ muscarinic receptors (Lee et al, 2005). The mechanism involves specific activation of the channels by $G\alpha_i$ subunits. Receptors coupled to $G\alpha_{i2}$ primarily activate TRPC4 and receptors coupled to $G\alpha_{i3}$ primarily activate TRPC5 in order to mediate the receptor-stimulated monovalent cation current and the Ca^{2+} influx.

Several studies have reported modulation of TRPC4 and TRPC5 activity by GTPγS-activated PTX-sensitive G-proteins and $G_{i/o}$-coupled receptors (Xu et al, 2006; Otsuguro et al, 2008; Jeon et al, 2008). Activation of TRPC4 by muscarinic receptor stimulation of GI smooth muscle was inhibited by PTX and was shown to be critical in evoking and regulating GI tract motility (Tsvilovskyy et al, 2009). Our results provide a molecular mechanism to explain the activation of TRPC4 by the PTX-sensitive G protein signaling. A unique feature of the m*I*CAT is that it requires simultaneous activation of both the M2 and M3 muscarinic receptors. Conversely, cationic channel activation in murine gut smooth muscle cells involves three separate pathways (Sakamoto et al, 2007). 1) The M3–$G\alpha_q$-PLCβ system, which transiently activates the 70-pS and 120-pS cationic channels concurrently with IP3-induced Ca^{2+} release. 2) The M2 pathway, which transduces signals from M2 receptors via $G\alpha_o$ to the 70-pS cationic channel and shifts the transient activation toward a longer open mode. 3) The M2/M3 pathway, which transmits M2 signals via $G\alpha_o$ and M3 signals via a $G\alpha_q$-independent PLC, to

the 70-pS cationic channel, resulting in a much longer open mode. The latter pathway does not work well when either the M2 or the M3 receptors are lacking or when either $G\alpha_o$ or PLC are inactivated. In addition, the M2/M3 pathway, but not the M2 or M3 pathway, involves processes in which Ca^{2+} has a potentiating effect on channel activation, suggesting that the M3 pathway may facilitate the function of the M2/M3 pathway through IP_3-induced Ca^{2+} release (Zholos et al, 1997). We argue that if the 70-pS channel is mediated by TRPC4, then the pathways involving the M2 receptors use $G\alpha_{i2}$ to directly activate the channel.

In addition to TRPC4/5, activation by the $G\alpha_{i/o}$ subunits have been reported to regulate several other TRP channels. For example, in G_o-coupled mGluR6, $G\alpha_o$ closes a downstream nonselective cation channel in ON bipolar cells that is mediated by TRPM1-L (Koike et al, 2010). Pheromone sensing in the vomeronasal organ (VNO) is mediated by V1R-G_i and V2R-G_o complexes that activate TRPC2 (Zhang et al, 2010). Whether activation of these channels is by direct interaction with $G\alpha_{i/o}$ subunits as shown here for TRPC4/TRPC5 remains to be determined.

Our findings indicate that regulation of TRPC4 and TRPC5 by G-proteins is more complex than previously assumed. The newly discovered mechanism for activation of TRPC4 and TRPC5 suggests that Ca^{2+} influx through these channels can be activated by several mediators depending on receptor stimulation. As reported before and shown in Figure 1, TRPC4 and TRPC5 can clearly be activated by $G\alpha_q$-coupled receptors and mediated by several of the mechanisms reported before. However, activation by $G\alpha_q$-coupled receptors appears to be modest (Figure 1). More significant activation of

TRPC4/5 is elicited by stimulation of $G\alpha_i$-coupled receptors that is mediated by direct activation of the channels by $G\alpha_i$ subunits. The $G\alpha_i$ binding domain in TRPC4 and TRPC5 shares binding motifs with other regulatory molecules (CIRB, SESTD1) in the C-terminal region of TRPC4 and TRPC5. Modeling and mutation analyses indicate that the ^{711}RNLVKR^{716} region is important for the interaction between $G\alpha_{i2}$ and TRPC4 (Figure S6). By contrast with GIRK channels, $G\beta\gamma$ subunits do not appear to be involved in the direct activation of TRPC4 or TRPC5 by $G\alpha_i$. It is likely that the major role of $G\beta\gamma$ is regulating channel function by sequestering $G\alpha_{i/o}$ subunits in the resting state. The mode of TRPC4/TRPC5 regulation by $G\alpha_{i/o}$ subunits reported here likely constitutes a major pathway in smooth muscle. It will be interesting to explore the full potential of this form of regulation in other cell types, particularly when the regulation by $G\alpha_{i/o}$-coupled receptors involves changes in cellular Ca^{2+}. Examples include acetylcholine-induced vasoregulation, lung microvascular permeability (Freichel et al, 2001; Tiruppathi et al, 2002) and the increase of 5-hydroxytryptamine 2 receptor-coupled GABA release in thalamic interneurons (Munsch et al, 2003). In summary, the present findings expand knowledge regarding signal transduction by cytoplasmic Ca^{2+} beyond the $G\beta\gamma$ to the $G\alpha$ subunits of $G\alpha_i$-coupled receptors. Moreover, our findings point to a signaling function that is activated rather than inhibited by $G\alpha_i$ proteins and add an important function to the repertoire of functions activated by $G\alpha_i$ subunits.

References

1. Bezzerides VJ, Ramsey IS, Kotecha S, Greka A, Clapham DE. Rapid vesicular translocation and insertion of TRP channels. Nature cell biology. 2004;6:709-20.

2. Blair NT, Kaczmarek JS, Clapham DE. Intracellular calcium strongly potentiates agonist-activated TRPC5 channels. The Journal of general physiology. 2009;133:525-46.

3. Clancy SM, Fowler CE, Finley M, Suen KF, Arrabit C, Berton F, et al. Pertussis-toxin-sensitive Galpha subunits selectively bind to C-terminal domain of neuronal GIRK channels: evidence for a heterotrimeric G-protein-channel complex. Molecular and cellular neurosciences. 2005;28:375-89.

4. Finley M, Arrabit C, Fowler C, Suen KF, Slesinger PA. betaL-betaM loop in the C-terminal domain of G protein-activated inwardly rectifying K(+) channels is important for G(betagamma) subunit activation. The Journal of physiology. 2004;555:643-57.

5. Flemming PK, Dedman AM, Xu SZ, Li J, Zeng F, Naylor J, et al. Sensing of lysophospholipids by TRPC5 calcium channel. The Journal of biological chemistry. 2006;281:4977-82.

6. Ford CE, Skiba NP, Bae H, Daaka Y, Reuveny E, Shekter LR, et al. Molecular basis for interactions of G protein betagamma subunits with effectors. Science. 1998;280:1271-4.

7. Freichel M, Suh SH, Pfeifer A, Schweig U, Trost C, Weissgerber P, et al. Lack of an endothelial store-operated Ca2+ current impairs agonist-dependent vasorelaxation in TRP4-/- mice. Nature cell biology. 2001;3:121-7.

8. Gross SA, Guzman GA, Wissenbach U, Philipp SE, Zhu MX, Bruns D, et al. TRPC5 is a Ca^{2+}-activated channel functionally coupled to Ca^{2+}-selective ion channels. The Journal of biological chemistry. 2009;284:34423-32.

9. Jeon JP, Lee KP, Park EJ, Sung TS, Kim BJ, Jeon JH, et al. The specific activation of TRPC4 by Gi protein subtype. Biochemical and biophysical research communications. 2008;377:538-43.

10. Kim BJ, Jeon JH, Kim SJ, So I. Role of calmodulin and myosin light chain kinase in the activation of carbachol-activated cationic current in murine ileal myocytes. Canadian journal of physiology and pharmacology. 2007;85:1254-62.

11. Kim BJ, Kim MT, Jeon JH, Kim SJ, So I. Involvement of phosphatidylinositol 4,5-bisphosphate in the desensitization of canonical transient receptor potential 5. Biological & pharmaceutical bulletin. 2008;31:1733-8.

12. Kim MJ, Jeon JP, Kim HJ, Kim BJ, Lee YM, Choe H, et al. Molecular determinant of sensing extracellular pH in classical transient receptor potential channel 5. Biochemical and biophysical research communications. 2008;365:239-45.

13. Kim MT, Kim BJ, Lee JH, Kwon SC, Yeon DS, Yang DK, et al. Involvement of calmodulin and myosin light chain kinase in activation of mTRPC5 expressed in HEK cells. American journal of physiology Cell physiology. 2006;290:C1031-40.

14. Kim YC, Kim SJ, Sim JH, Cho CH, Juhnn YS, Suh SH, et al. Suppression of the carbachol-activated nonselective cationic current by antibody against alpha subunit of Go protein in guinea-pig gastric myocytes. Pflugers Archiv : European journal of physiology. 1998;436:494-6.

15. Koike C, Obara T, Uriu Y, Numata T, Sanuki R, Miyata K, et al. TRPM1 is a component of the retinal ON bipolar cell transduction channel in the mGluR6 cascade. Proceedings of the National Academy of Sciences of the United States of America. 2010;107:332-7.

16. Lee KP, Jun JY, Chang IY, Suh SH, So I, Kim KW. TRPC4 is an essential component of the nonselective cation channel activated by muscarinic stimulation in mouse visceral smooth muscle cells. Molecules and cells. 2005;20:435-41.

17. Miehe S, Bieberstein A, Arnould I, Ihdene O, Rutten H, Strubing C. The phospholipid-binding protein SESTD1 is a novel regulator of the transient receptor potential channels TRPC4 and TRPC5. The Journal of biological chemistry. 2010;285:12426-34.

18. Miller M, Shi J, Zhu Y, Kustov M, Tian JB, Stevens A, et al. Identification of ML204, a novel potent antagonist that selectively modulates native TRPC4/C5 ion channels. The Journal of biological chemistry. 2011;286:33436-46.

19. Munsch T, Freichel M, Flockerzi V, Pape HC. Contribution of transient receptor potential channels to the control of GABA release from dendrites. Proceedings of the National Academy of Sciences of the United States of America. 2003;100:16065-70.

20. Ordaz B, Tang J, Xiao R, Salgado A, Sampieri A, Zhu MX, et al. Calmodulin and calcium interplay in the modulation of TRPC5 channel activity. Identification of a novel C-terminal domain for calcium/calmodulin-mediated facilitation. The Journal of biological chemistry. 2005;280:30788-96.

21. Otsuguro K, Tang J, Tang Y, Xiao R, Freichel M, Tsvilovskyy V, et al. Isoform-specific inhibition of TRPC4 channel by phosphatidylinositol 4,5-bisphosphate. The Journal of biological chemistry. 2008;283:10026-36.

22. Riven I, Iwanir S, Reuveny E. GIRK channel activation involves a local rearrangement of a preformed G protein channel complex. Neuron. 2006;51:561-73.

23. Roy A, Kucukural A, Zhang Y. I-TASSER: a unified platform for automated protein structure and function prediction. Nature protocols. 2010;5:725-38.

24. Sakamoto T, Unno T, Kitazawa T, Taneike T, Yamada M, Wess J, et al. Three distinct muscarinic signalling pathways for cationic channel activation in mouse gut smooth muscle cells. The Journal of physiology. 2007;582:41-61.

25. Sali A, Blundell TL. Comparative protein modelling by satisfaction of spatial restraints. Journal of molecular biology. 1993;234:779-815.

26. Schaefer M, Plant TD, Obukhov AG, Hofmann T, Gudermann T, Schultz G. Receptor-mediated regulation of the nonselective cation channels TRPC4 and TRPC5. The Journal of biological chemistry. 2000;275:17517-26.

27. Shi J, Mori E, Mori Y, Mori M, Li J, Ito Y, et al. Multiple regulation by calcium of murine homologues of transient receptor potential proteins TRPC6 and TRPC7 expressed in HEK293 cells. The Journal of physiology. 2004;561:415-32.

28. Shimizu S, Yoshida T, Wakamori M, Ishii M, Okada T, Takahashi M, et al. Ca^{2+}-calmodulin-dependent myosin light chain kinase is essential for activation of TRPC5 channels expressed in HEK293 cells. The Journal of physiology. 2006;570:219-35.

29. So I, Kim KW. Nonselective cation channels activated by the stimulation of muscarinic receptors in mammalian gastric smooth muscle. Journal of smooth muscle research = Nihon Heikatsukin Gakkai kikanshi. 2003;39:231-47.

30. Sung TS, Jeon JP, Kim BJ, Hong C, Kim SY, Kim J, et al. Molecular determinants of PKA-dependent inhibition of TRPC5 channel. American journal of physiology Cell physiology. 2011;301:C823-32.

31. Sung TS, Kim MJ, Hong S, Jeon JP, Kim BJ, Jeon JH, et al. Functional characteristics of TRPC4 channels expressed in HEK 293 cells. Molecules and cells. 2009;27:167-73.

32. Tang J, Lin Y, Zhang Z, Tikunova S, Birnbaumer L, Zhu MX. Identification of common binding sites for calmodulin and inositol 1,4,5-trisphosphate receptors on the carboxyl termini of trp channels. The Journal of biological chemistry. 2001;276:21303-10.

33. Tiruppathi C, Freichel M, Vogel SM, Paria BC, Mehta D, Flockerzi V, et al. Impairment of store-operated Ca^{2+} entry in TRPC4(-/-) mice interferes with increase in lung microvascular permeability. Circulation research. 2002;91:70-6.

34. Trebak M, Lemonnier L, DeHaven WI, Wedel BJ, Bird GS, Putney JW, Jr. Complex functions of phosphatidylinositol 4,5-bisphosphate in regulation of TRPC5 cation channels. Pflugers Archiv : European journal of physiology. 2009;457:757-69.

35. Tsvilovskyy VV, Zholos AV, Aberle T, Philipp SE, Dietrich A, Zhu MX, et al. Deletion of TRPC4 and TRPC6 in mice impairs smooth muscle contraction and intestinal motility in vivo. Gastroenterology. 2009;137:1415-24.

36. Xu SZ, Muraki K, Zeng F, Li J, Sukumar P, Shah S, et al. A sphingosine-1-phosphate-activated calcium channel controlling vascular smooth muscle cell motility. Circulation research. 2006;98:1381-9.

37. Xu SZ, Sukumar P, Zeng F, Li J, Jairaman A, English A, et al. TRPC channel activation by extracellular thioredoxin. Nature. 2008;451:69-72.

38. Yan HD, Okamoto H, Unno T, Tsytsyura YD, Prestwich SA, Komori S, et al. Effects of G-protein-specific antibodies and G beta gamma subunits on the muscarinic receptor-operated cation current in guinea-pig ileal smooth muscle cells. British journal of pharmacology. 2003;139:605-15.

39. Yoshida T, Inoue R, Morii T, Takahashi N, Yamamoto S, Hara Y, et al. Nitric oxide activates TRP channels by cysteine S-nitrosylation. Nature chemical biology. 2006;2:596-607.

40. Zhang P, Yang C, Delay RJ. Odors activate dual pathways, a TRPC2 and a AA-dependent pathway, in mouse vomeronasal neurons. American journal of physiology Cell physiology. 2010;298:C1253-64.

41. Zhang Y. I-TASSER server for protein 3D structure prediction. BMC bioinformatics. 2008;9:40.

42. Zholos AV, Bolton TB. Muscarinic receptor subtypes controlling the cationic current in guinea-pig ileal smooth muscle. British journal of pharmacology. 1997;122:885-93.

43. Zhu MH, Chae M, Kim HJ, Lee YM, Kim MJ, Jin NG, et al. Desensitization of canonical transient receptor potential channel 5 by protein kinase C. American journal of physiology Cell physiology. 2005;289:C591-600.

국 문 초 록

Transient Receptor Potential Canonical (TRPC) channels은 칼슘 투과성을 가진 비 선택적 양이온 통로로서 세포 내에서 수많은 기능을 담당하는 주요 이온 통로이다. TRPC 이온통로들의 활성화 기전으로서 $G\alpha_q$-PLC 경로가 주요한 세포 내 신호전달 기전으로 보고 되고 있다. 그럼에도 불구하고, $G\alpha_q$-PLC 경로가 TRPC4/5 이온통로들의 주요 활성화 기전인지에 대해서와 어떠한 기전을 통해 기타 Gα 단백질들이 이들 이온통로들을 조절하는지에 대해서는 보고되어 있지 않다. 선행연구결과에서, TRPC4/5가 $G\alpha_i$에 의해 활성화 될 수 있다는 현상이 보고되었으나, 활성화 기전은 제시되지 않았다. 본 논문에 제시된 결과를 통해 $G\alpha_i$ 아형들이 TRPC4/5의 직접적인 주요 활성화 인자임을 찾을 수 있었고, 특히 TRPC4의 활성화에는 $G\alpha_{i2}$가 TRPC5의 활성화에는 $G\alpha_{i3}$가 주요한 활성화 인자임을 관찰하였다. 또한 $G\alpha_{i/o}$와 결합하는 무스카린성 아세틸콜린 수용체(Muscarinic acetylcholine receptor)인 M2 수용체에 의해 TRPC4/5가 활성화되는 것이 관찰되었으며, 이 수용체와 GTPγS에 의한 TRPC4/5 이온통로의 활성화가 백일해독소(*Pertusis* Toxin)에 의해서 억제되는 현상을 관찰 할 수가 있었다. 더욱이, TRPC4/5 모두 두 이온통로의 C-terminal에 보존된 아미노산 서열인 SEC14-like and spectrin-type domains (SESTD)과 $G\alpha_i$ 아형 사이에서 직접적인 상호작용을 통해 활성화되는 결과가 관찰 되었다. structural modeling 결과를 통해서 TRPC4 C-말단에 존재하는 두 개의 아미노산 (lysine 715 and arginine 716)이 $G\alpha_{i2}$와의 상호작용을 매개하는 것이 동정되었다. 이러한 결과들을 통해서 TRPC4/5의 활성화를 유도하는 분자기전이 $G\alpha_i$와 TRPC4/5의 상호작용임을 결론지을 수 있다.

*** 본 내용은 미국 생화학회 학술지 (The Journal of biological chemistry, 2012; 287:17029-39)에 출판 완료된 내용임**

……

주요어 : TRPC, TRPC4, TRPC5, $G\alpha_{i2}$, $G\alpha_{i3}$, 비선택성 양이온 통로

학번 : 2009-30610